The Experimental UWB Link

Pawel Rulikowski, *Student Member, IEEE,* Vratislav Sokol, *Member, IEEE,*
Tomasz Waliwander, Julien Le Kernec

Centre of Adaptive Wireless Systems, Cork Institute of Technology, Department of Electronics,
Rossa Avenue, Cork, Ireland, Email: prulikowski@cit.ie, sokolv@fel.cvut.cz,
tomasz.waliwander@cit.ie, julienlekernec@gmail.com

***Abstract*—The experimental results from simple ultra wideband link are presented. The UWB link consisting of typical broadband microwave circuits built of commercially available components is able to send and detect unmodulated broadband electrical pulses with 20 MHz pulse repetition frequency. The system operates with approximately 60% of fractional bandwidth in 4GHz band with spectral density of -140dBW/Hz.**

***Index Terms*—Pulse generation, pulse shaping circuits, transient response, ultra wideband (UWB)**

I. Introduction

Recently, ultra wideband technology (UWB) has attracted many worldwide interest in many areas of research and commercial applications. Undisputable benefits of this emerging technology create new challenges in many aspects. Many traditional approaches to system and hardware design often fail when applied to UWB, therefore there is a need for modified or even new techniques.

The most widespread definition for UWB system seems to be that proposed by US Federal Communication Commission. This defines the UWB communication as any kind of communication that occupies more than 25% of fractional bandwidth or at least 500MHz as a nice gesture to industrial community. Even though this definition causes some controversy and misunderstanding it is the only one at the moment consistent. The Europe is still behind in terms of legislation but proposed by ETSI regulation quite well reflects American regulations. The FCC (and proposed ETSI) approved UWB mask is presented in Fig.1. The allowed frequency band spreads from 3.1 to 10.6 GHz giving enormous, never before accessible 7.5GHz of constant bandwidth. An allowed power spectral density is -41.3 dBm/MHz of Effective Isotropically Radiated Power (EIRP).

The UWB technology has some unique features that promise its utilization in many applications that hard or even it is not possible to realize in "traditional" narrowband technologies. Some of the unique features and applications include:

- UWB system is highly immune to multipath propagation phenomenon
- Able to provide 3D tracking capability with resolutions down to centimetres
- Power aware and efficient from power consumption point of view
- Extremely hard to eavesdrop
- Achievable high data rates (up to 500Mb/s) in short range communication with low power consumption (i.e. Bluetooth quality of service with 100 times less average power)
- Able to see through obstacles (often used as ground penetrating radars)

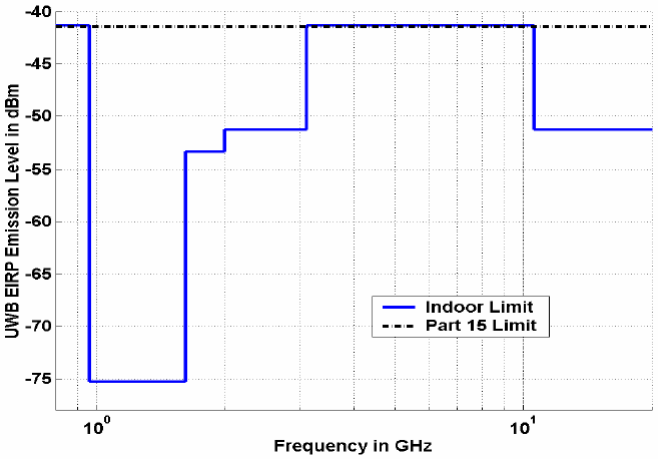

Fig.1. FCC approved UWB indoor mask.

The UWB systems are potentially interesting mainly for short range high data rate communication, precise location, power aware systems as sensor networks.

II. The Ultra Wideband Transceiver

A. General structure

An UWB system structure is illustrated in Fig.2. 20 MHz square wave crystal stabilized generator provides trigerring signal for a baseband pulse generator. The system exploits heterodyning principle for placing baseband pulse around the desired center frequency in our case 4GHz. Finally, the shaped pulse is supplied to the broadband antenna and transmitted.

Our receiver uses one of the simplest possible implementation of the UWB receiver – threshold detector. Such approach is not optimal but relatively simple in implementation. The received signal from antenna is amplified in a two stage amplifier – the first stage is LNA based on discrete pHEMT transistor and the second one uses a MMIC

broadband amplifier. In the next stage amplified signal is detected by a broadband threshold pulse detector.

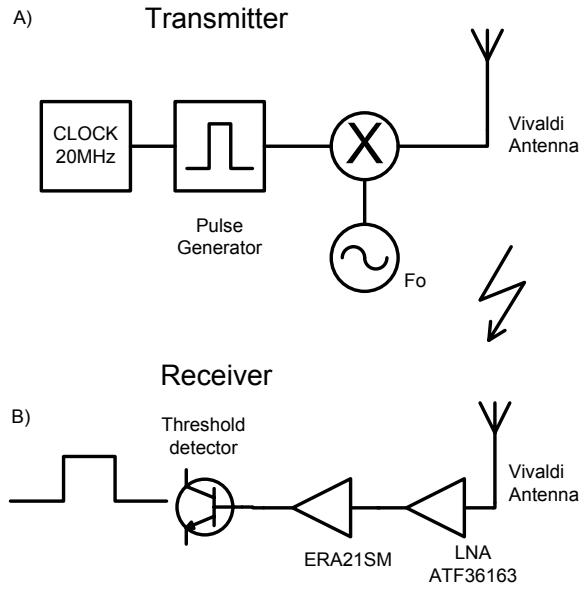

Fig.2. The experimental UWB link structure.

B. *Transmitter*

1) *Pulse generator*

The pulse generator used in our experiment uses as a step generator step recovery diode MA44769, that excited from the digital driver creates two balanced steps that are further shaped in distributed pulse shaping network to create short electrical pulse [4]. The detailed schematic is shown in Fig.3.

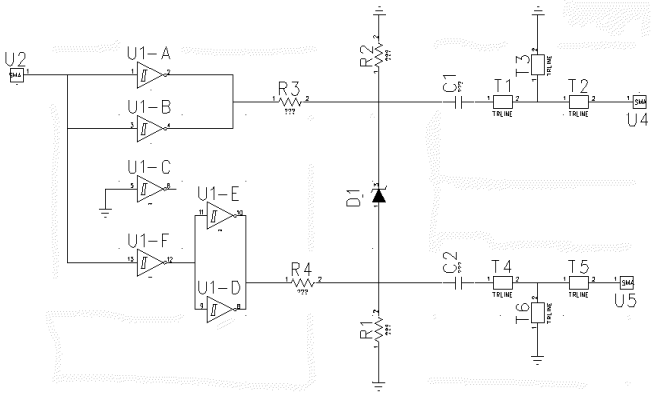

Fig. 3. The circuit diagram of balanced subnanosecond pulse generator.

A balanced "input generator – driver" was created using a CMOS buffer with a Schmitt type input (74ACT14) U1 in order to get balanced output from an unbalanced generator. The second function of the generator is to shorten rise time of square wave connected to input U2 from 50 ns down to 1 ns and provide source or sink current of ± 50 mA. When one group of gates U1-A, U1-B goes high, the other one U1-F, U1-E and U1-D drops it logic state down. Such connection results in changing polarization of the diode from forward to reverse state. The balanced driver combines two features in one – it both biases and triggers SRD generator. The pulse forming concept [1] is based on the division of a propagated wave over the transmission line between short circuited stub – T6 (T3), with impedance being half that of the main line, and the "main line" – T1, T2 (T4, T5) and use of occurring reflections to shape the output pulse. The generated pulse (parameters in Table I and time waveform in Fig.4) has a duration equal to twice that needed for propagation over the shorted stub and occurs at the output after time needed for propagation over T1 and T2 (T4, T5). The step generated by the SRD is fed into the pulse forming network through capacitor C1 (C2), which prevents current flowing to load during the digital driver steady state. The aim of the terminating resistors R1 and R2 is to match the transmission line junction point to 50 Ω and prevent further reflections of pulse thereby reducing ringing. The pulse generator consists of two identical sections of the pulse forming network used to achieve a balanced output as it is shown in Fig. 3. They were connected to the anode and cathode of the SRD. In order to obtain unbalanced to balanced transition the ground planes of the digital and microwave part of the pulse generator were separated. It is worth noting that the whole circuit uses only a single positive 5V bias voltage. This feature is extremely useful in portable and handheld applications, where negative biasing is often simply not accessible or requires use of DC-DC converters.

TABLE I
PULSES' PARAMETERS

Parameter	Distributed pulse forming network
Rise/fall time (10-90%)	168 ps
Pulse width (50-50%)	335ps
Pulse amplitude	±750 mV (10 dBm – peak power)

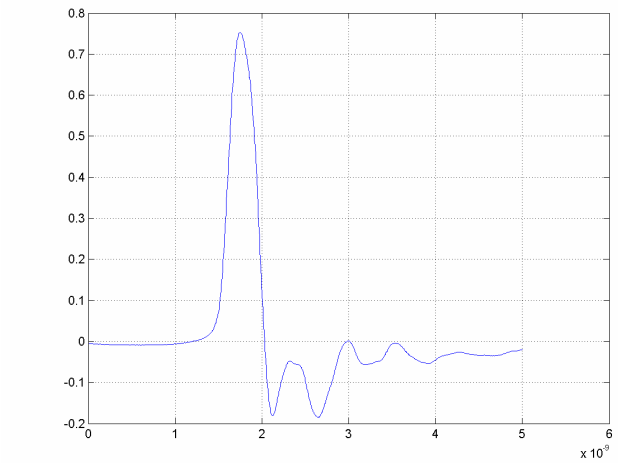

Fig.4. Time waveform of the positive pulse created with pulse shaping network.

2) *Mixer*

A mixer used for up-conversion of the baseband pulse was

double balanced type with broadband frequency characteristic from 2-8GHz. It is commercial LTCC mixer Mini-Circuits type MCA1-85. The layout created on Taconic Cer-10 (ε_r=9.5) 0.63mm thick organic substrate with 35μm double side copper cladding is presented in Fig. 5.

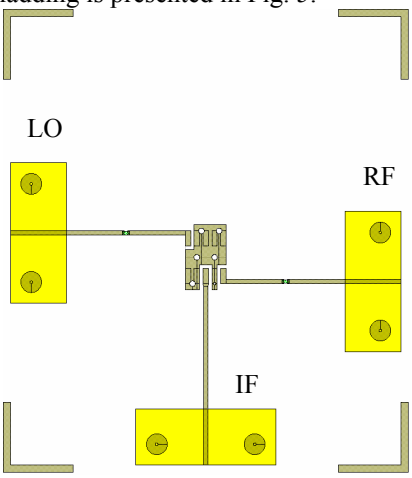

Fig.5. MCA1-85 mixer layout.

Block capacitors on the LO (left) and RF (right) were used to remove DC components from those signals. The IF port was fed by positive pulse from the pulse generator. The LO signal was supplied from HPE4433B signal generator. The RF port was used as the output port.

3) *Vivaldi antenna*

One critical part of the UWB communication link is the effect of the antenna on the transmitted pulse [2]. Thus the antenna should have minimal distortion on the transmitted pulse. The designed UWB antenna consists of three main parts that are microstrip impedance transformer, microstrip to slotline transition and Vivaldi antenna, see Fig.6. The designed UWB antenna has small dimensions 110x120mm.

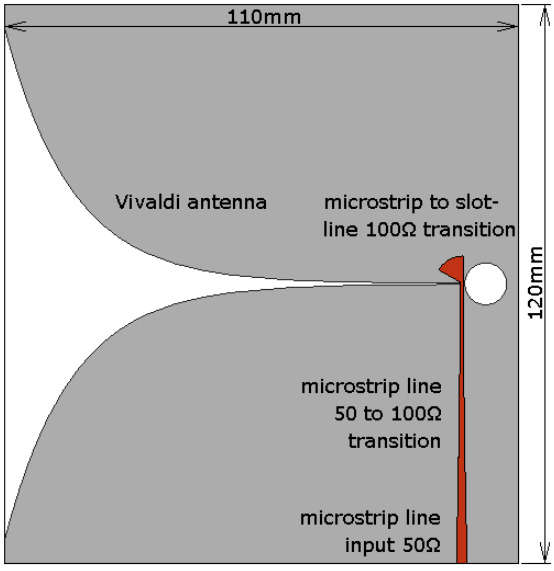

Fig.5. UWB Vivaldi antenna.

The Vivaldi antenna is excited via the microstrip to slotline transition, see Fig. 5. The transition construction exploits wideband features of a microstrip radial stub used as a virtual wideband short. Thus the microstrip is virtually shunted to the second half of the slotline metallization while the first half serves as a ground metallization for the microstrip line. Since the slot line is terminated by an open end the energy can propagate through transition without any reflection and insertion loss in an ideal case. Unfortunately, the real transition has insertion loss about 1.8 dB at 10.6 GHz, which is caused by radiation from the transition. The nominal line impedance 100 ohm was chosen as a trade off between radiation and slotline gap dimension at the transition. The angle of the radial stub is 60 degrees and the length was adjusted using Microwave Office® in order to obtain the reflection coefficient as close as possible to a short over the frequency band 3.1-10.6 GHz.

The antenna was designed on Taconic TLX-8 substrate (ε_r =2.55, h=0.76 mm, td=0.0019 at 10GHz). Results of the modeling of the antenna using CST MicroWave Studio® are shown in Fig. 7 and Fig.8.

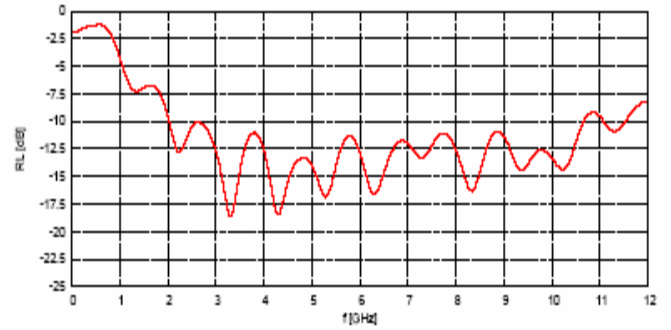

Fig.7. Simulation of the return loss of the designed Vivaldi antenna.

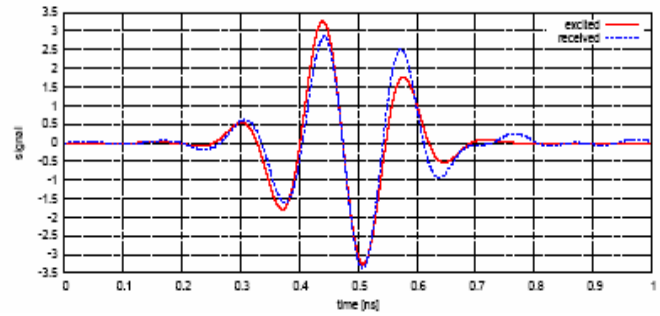

Fig.8. An UWB pulse distortion caused by antenna.

C. *Receiver*

1) *Receiving antenna*

The antenna used at the reception side is of Vivaldi type the same type as that used in the transmitter.

2) *Low noise amplifier*

Low noise amplifier is one of the most important elements of UWB receiver. Its aim is to amplify very weak

(-100dBm/MHz of power spectral density) and broadband incoming signal, which appears at antenna's aperture, to the appropriate level which ensures non-problematic detection and retrieving the data. Moreover, since the power spectral density of UWB pulse just detected by the antenna is very low, broadband amplifier has to contribute as low noise energy to the amplified signal as possible. Therefore LNA for the UWB receiver has to meet some particular requirements, for instance: low-noise figure, high gain, good input and output matching and constant group delay in order to give amplified non-distorted signal. Those parameters have serious influence in the overall sensitivity of the receiver. Since UWB transceiver is tend to be employed in the remote devices, it has to have low power consumption.

Low noise amplifier employed in our system was design to reach the lowest possible NF. The Agilent ATF-36163 transistor was chosen mainly because provides NF less than 1 dB with associated high gain (16 – 12 dB) in the frequency range of 3-8 GHz. The amplifier was designed with the aid of Microwave Office® CAD tool, on Taconic CER-10 substrate with thickness 0.635 mm and 35 μm for dielectric substrate and copper metallization layers, respectively. The final amplifier layout is shown in Fig.9.

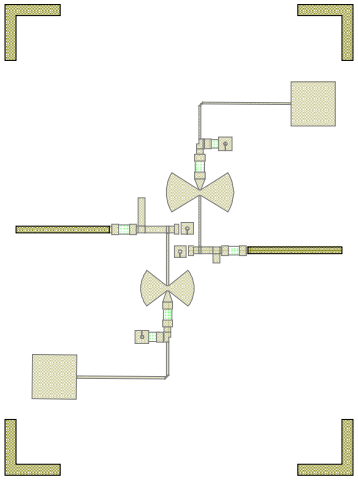

Fig.9. Layout of the low noise amplifier.

Drain and gate biasing networks were designed to reduce leakage of the RF signal to the DC power supply circuit and to give negligible effect on the overall gain of the amplifier. They were designed to provide good isolation in the whole UWB frequency range regulated by FCC. In Fig.10 frequency response of drain biasing circuit is shown.

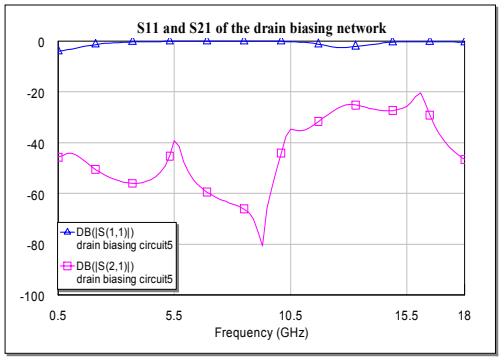

Fig.10. Frequency response of the drain biasing network.

Both biasing networks consist of the narrow 75 Ω characteristic impedance microstrip line followed by double radial stub and 210 Ω (drain) or 50 Ω (gate) resistors. The 1 nF capacitor shunts the RF signal to the ground. Utilization of double radial stubs provides better isolation in the frequency band of interest.

Input matching network was designed to provide the lowest possible NF in the range of 3-8 GHz, while output network gives best power matching. Simulated gain and NF of the amplifier are given in Fig.11.

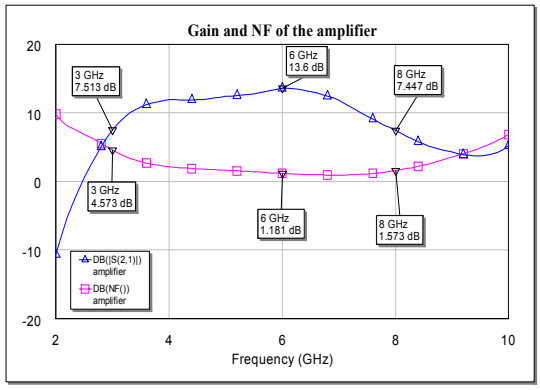

Fig.11. Simulated gain and noise figure of the amplifier.

The measurements taken with Rhode & Schwarz spectrum analyzer FSU 26 are shown in Fig.12.

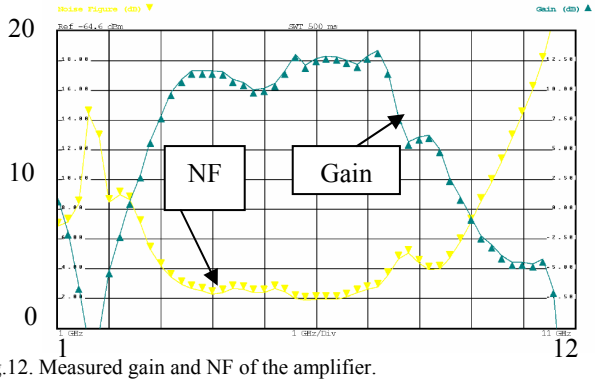

Fig.12. Measured gain and NF of the amplifier.

3) *The second amplifier*

The second stage of the amplifier was realized by MMIC commercially available, surface mount broadband amplifier ERA21SM. The measured frequency response in range from 1-11GHz of the amplifier mounted on Taconic Cer-10 substrate is shown in Fig.13.

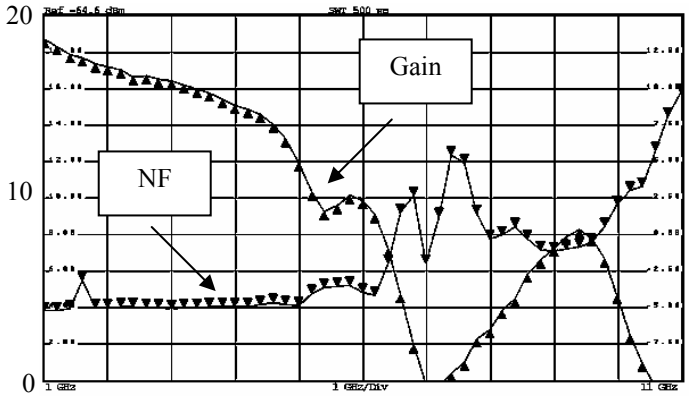

Fig.13. Measured ERA21SM gain and noise figure.

4) *Pulse detector*

The concept of the detector is based on fast monostable flip-flop circuit that provides strong positive feedback [3]. Therefore, a fast time response to the input pulse can be expected. A schematic diagram of the detector model is depicted in Fig.14.

The first stage of the detector, containing transistor Q1, shapes an arbitrary input pulse to one negative trigger peak. This is illustrated in Fig.15 . This negative peak triggers the following monostable flip-flop circuit consisting of transistors Q2 and Q3. In order to minimize the influence of load impedance on the monostable flip-flop circuit the buffer transistor Q4 is placed at the end. The measured response of the detector is presented in Fig. 16.

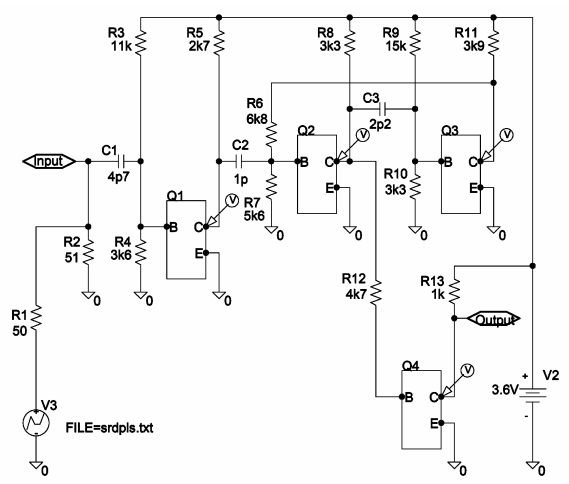

Fig.14. Spice model of the pulse detector. Subcircuit Q1-Q4 contains Gummel-Poon model of bipolar transistor BFG 410 W including parasitic elements of its package SOT343R.

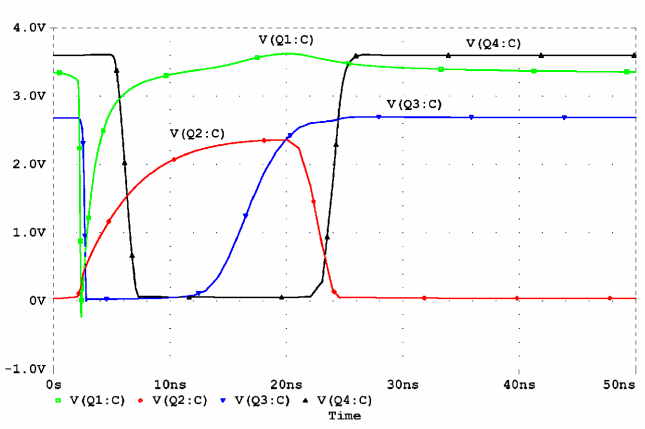

Fig. 15. Simulated waveforms of the pulse detector.

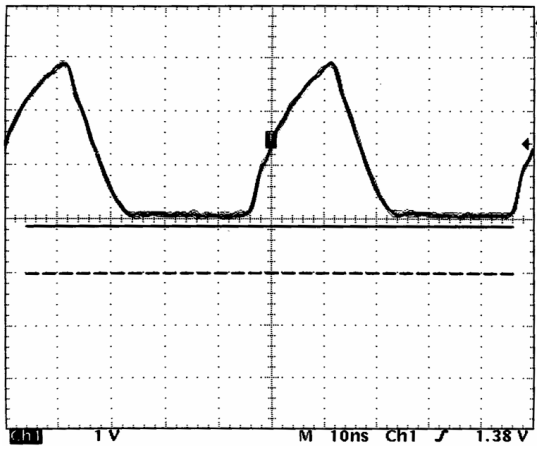

Fig.16. Measured waveform at the detector output for the PRF=20 MHz and the attenuation 6 dB (positive peak value 329 mV) of the excitation pulse.

III. THE UWB LINK MEASUREMENTS

The measurements of the UWB link were carried out with the setup presented in Fig.2. At the beginning performance of the mixer as a fast multiplier has been checked. Pulse of the parameters presented in Table I and waveform in Fig.4 was used as a baseband switching signal and provided to IF mixer input. The RF frequency was supplied from the signal generator set to 3.9 GHz and power of 10d Bm. The output signal was supplied directly to Vivaldi antenna. Fig.17 presents waveforms of the signals in time and frequency domain. In Fig.17a) spectrum of the baseband signal is shown – useful -10dB bandwidth spreads from DC up to above 2 GHz with the power spectral density -122 dB/Hz around 0.5 GHz. The up-converted pulse and its spectrum can be seen in Fig. 17b) and c) respectively. The RF burst lasts for around 0.7ns and has the center frequency of the 3.9 GHz as it is presented in Fig.17c). The maximum PSD is -137 dB/Hz (FCC allows -131dB/Hz), -10 dB bandwidth covers frequencies from 2.8-5.2GHz giving 61% of fractional bandwidth (FCC requires at least 25%). Peak to peak values of the received signal over short distances, mainly because of the limitations of the low gain of the used amplifiers and the length of the connecting cables, are gathered in Table II.

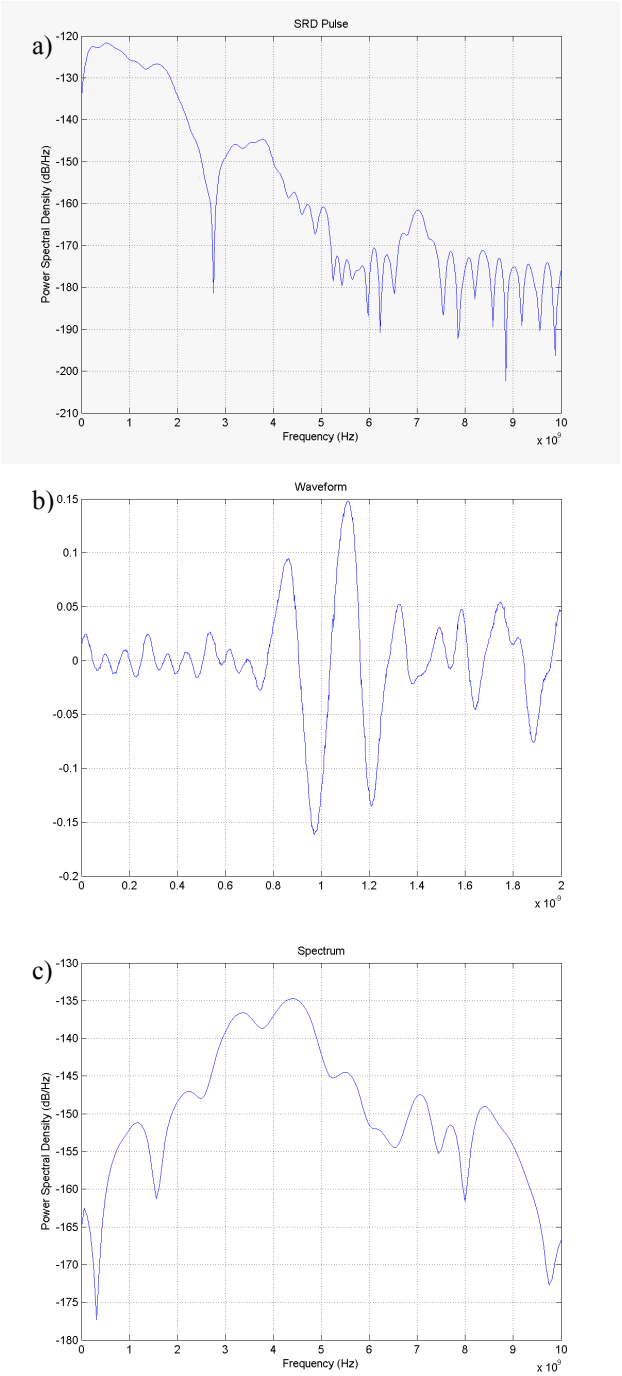

Fig.17. a) Baseband pulse spectrum, b) UWB pulse waveform after mixer, c) UWB signal spectrum.

TABLE II

RECEIVED SIGNAL AMPLITUDE VS DISTANCE

Distance [cm]	Peak to peak voltage at the input of the detector [mV]
33	457
27	562
22	670
19	721

V. CONCLUSION

The principles of UWB link has been tested with the designed in house setup. Simple arrangement proves low complexity of the UWB transceiver. Even though the experiment does not take into account such issues as multiple access to the medium, synchronization etc. it shows that hardware arrangement promises low cost, low complex radio for future applications with respectable data rates.

ACKNOWLEDGMENT

This work, part of the M-Zones Project (www.m-zones.org) has been supported under the Programme for Research in Third Level Institutions (PRTLI) by Irish Higher Education Authority (HEA).

REFERENCES

[1] G. F. Ross "The Synthetic Generation of Phase-coherent Microwave signals for Transient Behaviour Measurements", *IEEE MTT Transactions,*1965, 704-705

[2] P.Piksa, V.Sokol, "Small Vivaldi Antenna for UWB", internal report, CIT 2005

[3] V. Sokol, P. Rulikowski and J. Barrett, "Low Power Consuming Pulse Detector", submitted for publication at 2005 IEEE International Conference on Ultra-Wideband, Zurich 2005

[4] P. Rulikowski and J. Barrett, "Truly Balanced Step Recovery Diode Pulse Generator with Single Power Supply," *in IEEE RAWCON Conference Proc.*, Atlanta 2004